Model for phase equilibria in micellar solutions of nonionic surfactants

Raymond E. Goldstein
Cavendish Laboratory, Cambridge, CB3 OHE England and Laboratory of Atomic and Solid State Physics,[a]
Cornell University, Ithaca, New York 14853-2501

(Received 4 November 1985; accepted 6 December 1985)

The formation of spherical micelles in aqueous solutions of nonionic surfactants and the equilibria between two such micellar phases are studied with a phenomenological model incorporating hydrophobic interactions and the configurational entropy of the amphiphiles. The distribution of micelle sizes is determined over the entire temperature-composition phase diagram, and moments of that distribution function determine the consolute point parameters. In a generalization of an analysis given by Stillinger and Ben-Naim, the mathematical properties of various thermodynamic functions in the neighborhood of the critical micelle concentration are related to the location of branch points of the osmotic pressure in the complex concentration plane. The model attributes the experimentally observed lower critical solution points in these systems to surfactant–water hydrogen bonding, whose temperature dependence is described with a mean field approximation. Calculated phase diagrams are in qualitative agreement with those from experiments, in particular, exhibiting closed solubility loops with quite distinct upper and lower critical compositions, and values for the lower critical composition on the order of several percent volume fraction. The relevance of certain aspects of the model to the understanding of microemulsions is discussed.

I. INTRODUCTION

Recent light- and neutron-scattering experiments[1–4] in conjunction with phase equilibria studies[5,6] have shown that nonionic surfactants in aqueous solutions often form roughly spherical micelles of well-defined aggregation number, and that when two isotropic phases coexist, they are *both* micellar. It thus appears that the phase separation transition is like that in a simple binary mixture, with the *micelles* and the solvent as the two "species." Yet, these aggregates are polydisperse, and continually exchanging particles with each other through a multitude of chemical equilibria, so the description of phase equilibria takes on added complexity.[7]

The connection between aggregation and phase equilibria in micellar solutions has been studied by Blankschtein, Thurston, and Benedek,[8] with application to systems in which the structure of the free energy hierarchy for aggregate formation is particularly simple. In the present paper, we investigate by similar methods the phase equilibria in micellar solutions of a particular class of nonionic surfactants, but using a phenomenological model for the micelle free energy which is rather more detailed in its description of the aggregates. That micelle free energy, described in Sec. II, incorporates certain polymer chain entropy effects suggested by de Gennes,[9] and studied in more detail by Leibler, Orland, and Wheeler,[10] but the present work differs conceptually in an important way from the latter, a point to which we return in Sec. V. In describing the nonideality of the solutions, we explore in detail a possible correspondence[11] between these micellar systems and conventional polymer solutions.[12] The micelle size distribution function is determined (numerically) over the whole phase diagram, and we exhibit the "fractionation" of the distribution in the two-phase region. These results also give insights into the characteristic forms of polydispersity in these systems, an important consideration in the interpretation of scattering experiments.

Section III is a discussion of the mathematical structure of thermodynamic quantities in the neighborhood of the critical micelle concentration (cmc), and is based on work by Stillinger and Ben-Naim[13] showing a correspondence with the Lee–Yang[14] theory of phase transitions. We find that the solution properties near the cmc can be related to the branch points of the osmotic pressure in the plane of complex monomer concentration.

In systems such as the alkyl polyoxyethylene ethers,[5,6] and also in a variety of related multicomponent microemulsions (oil + water + surfactant),[15–17] the liquid–liquid phase equilibrium is "reentrant," in that the consolute point is the *lower* extremum of the coexistence curve, so that a macroscopically disordered (one-phase) region exists at a temperature which is lower than that of the ordered two-phase domain. In binary and pseudobinary mixtures of comparable-size molecules, such *reentrant solubility* has been attributed[18,19] to entropic effects associated with hydrogen bonding between unlike components. We adopt that explanation in the present work, utilizing a mean field description[20] of such transitions. As shown in Sec. IV, the resultant phase diagrams are in qualitative agreement with experiment, particularly with respect to the existence of closed solubility loops with quite different upper and lower critical compositions. In future work we shall explore quantitative comparisons.

The form of the free energy density discussed in Secs. II and III has aspects in common with the modification of the Talmon–Prager[21] model for microemulsions studied recently by de Gennes *et al.*[22,23] and Widom.[24] In both the present model and the model microemulsion the free energy of the solution has minima at different "domain" sizes, and the competition between these minima determines the observed

---

[a] Present address.

aggregate size. In the micelle model that free energy surface is "populated" according to a mass-action relation, which is itself the result of a free energy minimization condition applied to the aggregate *size distribution function*. In contrast, in the model microemulsion, the free energy is minimized with respect to the *domain size* itself. In Sec. V we comment on the consequences of these two viewpoints on the continuity of certain thermodynamic properties. In particular, it is suggested that consideration of an equilibrium between members of a distribution of domain sizes may eliminate certain apparently unrealistic features[24] of the model microemulsion.

Finally, in Sec. VI we assess the model and briefly indicate directions in which it may be refined to complete the description of certain aspects of the observed temperature-composition phase diagram of the surfactant solutions, including the transitions to the various liquid crystalline phases.

II. THEORY

A. Free energy

We consider nonionic surfactants composed of a total of M elementary units, each with microscopic length a, of which $M/2$ are hydrophilic and $M/2$ are hydrophobic. The more general case of unequal head and tail lengths is easily studied by a simple modification of the following. These two groups are arranged in diblock form, as in amphiphiles such as the alkyl polyoxyethylene ethers $C_iE_j\,[=\mathrm{CH_3(CH_2)}_{i-1}(\mathrm{OCH_2CH_2})_j\mathrm{OH}]$. The solution is composed of a total of N_p such polymers, and N_s solvent (water) molecules, the latter of which are also assumed to have the same microscopic size a. As a consequence of hydrophobic interactions the amphiphiles may aggregate into micelles with a range of aggregation number n, and we assign to each micelle a volume v_n equal to the sum of those of its constituent polymers, so $v_n = nMa^3$. The solution volume V is modeled as the sum of those of its constituents, $V = a^3(N_s + MN_p) = \Omega a^3$, where Ω is the total number of "sites" if we were to use a lattice model for the solution. The total volume fraction of polymer ϕ_p, which we choose as the fundamental composition variable ϕ, is $MN_p/(N_s + MN_p)$, and by mass conservation, $MN_p = \Sigma_n\, nMN_n$, and $\phi = \Sigma_n\, \phi_n$, where ϕ_n is the volume fraction of n-mers.

The contribution to the solution free energy arising from the translational entropy of the aggregates and solvent is estimated in the ideal solution approximation, with each component moving in a volume Ω,

$$F_t = k_B T\left[N_s \ln(N_s/\Omega) + \sum_{n=1}^{\infty} N_n \ln(N_n/\Omega)\right], \quad (1a)$$

which, when expressed as a free energy density $f_t = F_t/\Omega$ gives

$$f_t = k_B T\left[(1-\phi)\ln(1-\phi) + \sum_{n=1}^{\infty} (\phi_n/nM)\ln(\phi_n/nM)\right]. \quad (1b)$$

This is equivalent to the well-known Flory–Huggins[12,25] approximation for polymer solutions in which there is a distribution of "polymerization indices" nM. The translational free energy of *mixing* differs from Eq. (1b) by the substitution of the term $\ln(\phi_n)$ for $\ln(\phi_n/nM)$ in the summation, and its use in the expression for the total free energy, in place of Eq. (1b), corresponds[8] to absorbing a term $k_B T \ln(nM)$ into the standard chemical potential of an n-mer: We choose to exhibit that contribution explicitly. Although originally derived in the context of solution theory for long, flexible polymers, Eq. (1) may also be derived[26] on the basis of simple approximations to excluded volume effects, rather than from detailed specification of the geometry of the particles. Since this form of the translational entropy differs from the ideal gas approximation typically used in aggregation theory[27]:

$$F_t^{\mathrm{id}} = k_B T\left[N_s \ln(X_s) + \sum_{n=1}^{\infty} N_n \ln(X_n)\right], \quad (2)$$

where $X_s = N_s/(N_s + \Sigma_n N_n)$ and $X_n = N_n/(N_s + \Sigma_m N_m)$ are the number fractions of solvent and n-mers, respectively, the law of mass action derived herein will also differ. The use of the entropy of mixing in Eq. (1), rather than that from the ideal mixture approximation, explicitly accounts for the solute–solvent size asymmetry, which plays an important role in the determination of the asymmetry of the coexistence curve itself (*vide infra*).

The total free energy F of the solution is taken to be the sum of the above translational entropy of mixing, and terms which describe the internal free energy of the clusters and solvent, and their interactions. This internal contribution is

$$F_0 = N_s \mu_s^0 + \sum_{n=1}^{\infty} N_n \mu_n^0, \quad (3)$$

with μ_s^0 and μ_n^0 the standard chemical potentials of solvent and n-mers, defined in a system without interaggregate interactions.

In the spirit of a mean field theory, the contribution to the total free energy due to interactions between the various entities in solution, F_{int}, is estimated in a random mixing approximation so that

$$\begin{aligned} F_{\mathrm{int}} &= d\,[N_s(1-\phi)f_{ss} + MN_p\phi f_{pp} + 2N_s\phi f_{ps}] \\ &= \Omega d\,[(1-\phi)^2 f_{ss} + \phi^2 f_{pp} + 2\phi(1-\phi)f_{ps}]. \quad (4) \end{aligned}$$

Here, d is one-half the local coordination number, and equals the spatial dimensionality in a cubic lattice model of the solution. The f_{ij} are the microscopic interaction energies (or more generally free energies) associated with the interactions of the various species, and to describe systems with lower critical solution points these quantities must have a particular temperature dependence, as described more fully in Sec. IV. Since the surfactants considered have two distinct blocks, the polymer–polymer and polymer–solvent energies f_{pp} and f_{ps} are themselves averages of the hydrophilic and hydrophobic interactions.

With the total free energy $F = F_t + F_0 + F_{\mathrm{int}}$, the chemical potentials of the solvent and n-mers are, respectively,

$$\mu_s = (\partial F/\partial N_s)_{T,p,\{N_n\}}$$
$$= \mu_s^0 + k_BT\Big[\ln(1-\phi) + \phi - \sum_{m=1}^{\infty}\phi_m/mM\Big] - w\phi^2 + w_{ss}\,, \quad (5)$$

$$\mu_n = (\partial F/\partial N_n)_{T,p,\{N_{m\neq n}\}}$$
$$= \mu_n^0 + k_BT\Big[\ln(\phi_n/nM) - (1-\phi)Mn + 1 - nM\sum_{m=1}^{\infty}\phi_m/mM\Big] - nMw(1-\phi)^2 + nw_{pp}\,, \quad (6)$$

where $w_{ij} = df_{ij}$, and $w = w_{pp} + w_{ss} - 2w_{ps}$. The constant term w_{ss} in Eq. (5) effects neither the aggregation processes nor the phase equilibria, and may therefore be absorbed into μ_s^0, as we do.

The equilibrium distribution of micelle sizes $\{N_n\}$ is that which minimizes F, and, by mass conservation, that extremization condition is fulfilled by the relation

$$n\mu_1 = \mu_n\,. \quad (7)$$

This yields a mass-action relation

$$(\phi_n/M) = n(\phi_1/M)^n \exp[-\beta\Delta_n]\,, \quad (8)$$

with

$$\Delta_n = (\mu_n^0 + k_BT) - n(\mu_1^0 + k_BT)\,. \quad (9)$$

In the mean field approximation to the interactions the effects of interaggregate interactions are absent at the level of the mass action relation [Eq. (8)], although they may be present indirectly through a mechanical instability leading to phase separation. In general, of course, such interactions may significantly alter the distribution law, and their effect has been studied perturbatively.[28–30]

B. Free energy of the micelles

The micelles are assumed to be spherical, with a well-defined hydrocarbon "core" in which all of the surfactant hydrocarbon tails reside and whose density is uniform. Thus, if R_c is the radius of that core, we have the relation $(4\pi/3)R_c^3 = (M/2)na^3$ between the aggregation number and the core size. We write the chemical potential difference in Eq. (9) as $n\delta$, where δ is the free energy difference per surfactant molecule. The quantity Δ_n is itself composed of three terms which may be labeled "bulk," "surface," and "entropic": $\Delta_n = n\delta = n(\delta_b + \delta_s + \delta_e)$.

The bulk term δ_b is the main driving force for the aggregation, and reflects the favorability of transferring the hydrocarbon parts of the surfactant chains from the aqueous environment to the micelle core, and also the free energy change due to the proximity of the hydrophilic sections. This term is proportional both to the number of chains per aggregate and to the chain size;

$$n\delta_b = hMn\,, \quad (10)$$

where $h < 0$. A detailed theory would account for the dependence of h on the relative lengths of the hydrophobic and hydrophilic section of the amphiphiles. In later discussions we employ the dimensionless $\epsilon = -h/k_BT$, and on the basis of previous studies[27] of micelle formation, we expect that ϵ is typically of order unity. The known characteristics of hydrophobic interactions[31] suggest that the dominant contribution to h is entropic, and in numerical calculations we model its temperature dependence as $h = a - bT$, with $a(>0)$ and $b(>0)$ the enthalpic and entropic contributions, respectively.

The residual hydrocarbon–solvent and hydrophilic–hydrophobic interactions occur at the surface of the core and are characterized by a surface free energy per unit area τ. Their contribution to Δ_n is proportional to the core surface area $4\pi R_c^2$, thus,

$$n\delta_s = \gamma(Mn)^{2/3}\,, \quad (11)$$

where $\gamma = (9\pi)^{1/3}\tau a^2$. The dimensionless γ/k_BT is denoted by σ, and is of the same order as ϵ.

Returning to the mass action relation [Eq. (8)] it is clear that the two competing factors which determine the size distribution function are (i) the loss of entropy due to localization of the surfactant chains, as reflected in the $(\phi_1)^n$ term, and (ii) the gain in free energy upon aggregation, given by Δ_n. Yet, the surfactant chains in a micelle are significantly ordered, so that the entropic loss upon aggregation cannot be described entirely by the "center of mass" term (i). Clearly, as the mean size of the micelle increases, so too does the average elongation of the hydrocarbon tails, with an associated loss of configurational entropy. This higher order of the surfactants has been seen in recent simulations[32] and magnetic relaxation studies.[33]

In order to estimate this entropic contribution to Δ_n, we compare the entropies of a free chain and one whose mean extension is equal to the core radius,[9] under the simplifying assumption that the surfactants can be described as ideal random walk chains. The probability distribution function $P(r)$ for the end-to-end distance of a random-walking chain is a Gaussian[34]:

$$P(r) = \text{const}\exp[-3r^2/2R_0^2]\,, \quad (12)$$

where $R_0 = (M/2)^{1/2}a$ is the average extension of an ideal chain of fully extended length $(M/2)a$. The entropy as a function of the chain extension is $S(r) = k_B\ln[P(r)]$, so the change in free energy of n chains upon aggregation is

$$n\delta_e = -nk_BT\{\ln[P(R_c)] - \ln[P((M/2)^{1/2}a)]\}$$
$$= nk_BT[cn^{2/3}/M^{1/3} - 3/2]\,, \quad (13)$$

with c a purely geometric factor which is of order unity. In light of the simplicity of this estimate for the entropy loss, we use a value of unity in the numerical calculations. For the relatively short hydrocarbon chains found in the nonionic surfactants, we should not expect the ideal random-walk statistics strictly to be applicable, but the important loss of configurational entropy as the chains elongate is captured in this approximation. Since the surfactant chains are described with a Gaussian probability distribution lacking a cutoff at the fully extended length of the hydrocarbon tails, the free energy in principle permits unphysically large values for the

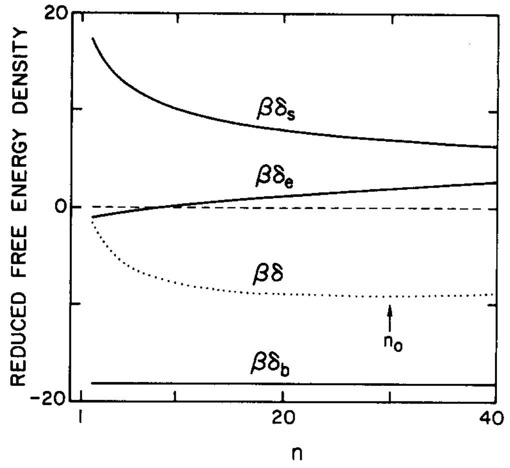

FIG. 1. Contributions to the micellar free energy per surfactant for $M = 20$, $\epsilon = 0.9$, and $\sigma = 3$. The minimum occurs at n_0, which is larger than the value at which the surfactant hydrocarbon chains are relaxed ($\delta_e = 0$).

micelle size. We find, however, that for all reasonable values of the bulk and surface parameters in the model, the aggregate size distribution is vanishingly small at these aggregation numbers, so the model is internally consistent. At large values of the surfactant concentration it is likely that micelle shapes other than spherical become important, especially in light of the variety of liquid crystalline phases observed[5,6] in the surfactant solutions. We elaborate on this point in Sec. VI.

In the absence of effects from the translational entropy terms [Eq. (1)] the optimum size of a micelle will be that aggregation number, n_0, which minimizes the free energy density

$$\delta = hM - (3/2)k_BT + \gamma M^{2/3}/n^{1/3} + k_BTcn^{2/3}/M^{1/3}\,. \tag{14}$$

Figure 1 shows δ/k_BT and its three contributions for a representative set of parameters. There is a shallow minimum of the free energy density at an aggregation number

$$n_0 = (\gamma/2ck_BT)M\,, \tag{15}$$

at which the loss of surfactant configurational entropy is balanced against the tendency to reduce the surface area per surfactant. From Eq. (15) we see that the mean core radius is proportional to $M^{2/3}$, so that the chains are stretched with respect to their mean length.[9,10]

We shall find that the micelles only approach the preferred size n_0 in the limit of large surfactant concentration, for then the translational entropy effects are at a minimum. Even at high surfactant concentration, and especially for lower ϕ, the mean size can be a sensitive function of h (Sec. III). That the average aggregation number should be less than n_0 is a consequence of the increase of translational entropy, hence decrease in free energy, associated with transferring surfactant from micelles to solution.

C. Phase equilibrium

If we regard the micellar solution as a multicomponent system, solvent plus micelles (with all possible aggregation numbers), we require that in two coexisting phases α and β of differing surfactant concentrations, ϕ_α and ϕ_β, at temperature T and pressure p, the chemical potential of the solvent takes on a common value,

$$\mu_s(\phi_\alpha,T,p) = \mu_s(\phi_\beta,T,p)\,, \tag{16}$$

as does that of each of the members of the micelle size distribution,

$$\mu_n(\phi_\alpha,T,p) = \mu_n(\phi_\beta,T,p) \quad (n \geqslant 1)\,. \tag{17}$$

By the extremum condition which leads to the mass action relation, Eq. (17) will be satisfied for all n if it holds for μ_1 in the two phases, and thus, as in conventional binary mixtures, there are only two independent chemical potentials in the associating solution. For this reason, the phase coexistence analysis is greatly simplified compared to that in *nonassociating* multicomponent systems.[35]

To determine the spinodal and critical point for the aggregating system, we thus apply the usual criteria for a two-component system, namely that with $\pi = [\mu_s(\phi = 0) - \mu_s(\phi)]/k_BT$ the reduced osmotic pressure, then

$$\partial\pi/\partial\phi = 0\,, \tag{18}$$

on the spinodal curve and, in addition, at the critical point,

$$\partial^2\pi/\partial\phi^2 = 0\,. \tag{19}$$

From the expression for the solvent chemical potential [Eq. (5)] these conditions are, respectively,

$$2\chi\phi - \phi/(1-\phi) - \sum_{n=1}^{\infty} (\partial\phi_n/\partial\phi)/nM = 0 \tag{20}$$

and

$$2\chi - 1/(1-\phi)^2 - \sum_{n=1}^{\infty} (\partial^2/\phi_n/\partial\phi^2)/nM = 0\,, \tag{21}$$

where $\chi = -w/kT$ is the Flory–Huggins mixing parameter. The derivatives are found from the law of mass action [Eq. (8)],

$$\frac{\partial\phi_n}{\partial\phi} = \left(\frac{1}{\phi_1}\frac{\partial\phi_1}{\partial\phi}\right) n\phi_n \tag{22}$$

and

$$\frac{\partial^2\phi_n}{\partial\phi^2} = \left[\left(\frac{1}{\phi_1}\frac{\partial^2\phi_1}{\partial\phi^2}\right) - \left(\frac{1}{\phi_1}\frac{\partial\phi_1}{\partial\phi}\right)^2\right] n\phi_n + \left(\frac{1}{\phi_1}\frac{\partial\phi_1}{\partial\phi}\right)^2 n^2\phi_n\,. \tag{23}$$

Differentiating the mass conservation equation $\phi = \Sigma_n\,\phi_n$ with respect to ϕ we obtain

$$\frac{1}{\phi_1}\frac{\partial\phi_1}{\partial\phi} = \frac{M}{\phi\langle Mn\rangle}\,, \tag{24}$$

and a further differentiation then gives

$$\frac{1}{\phi_1}\frac{\partial^2\phi_1}{\partial\phi^2} = [M^2\langle Mn\rangle - M\langle (Mn)^2\rangle]/\phi^2\langle Mn\rangle^3\,, \tag{25}$$

where angular brackets stand for a *mass fraction moment*

$$\langle \cdots \rangle = \sum_{n=1}^{\infty} (\cdots)[nMN_n/MN_p] = \sum_{n=1}^{\infty} (\cdots)\,\phi_n/\phi\,. \tag{26}$$

We thus reduce Eq. (18) to the simple form

$$2\chi\phi - \phi/(1-\phi) - 1/\langle Mn\rangle = 0\,, \tag{27}$$

which is that of a polymer solution *with a degree of polymerization equal to the weight-average size of the micelles.* Of course, $\langle Mn\rangle$ is itself a function of temperature and composition through the law of mass action.

The critical point equation

$$2\chi - 1/(1-\phi)^2 + [\langle (Mn)^2\rangle - \langle Mn\rangle^2]/\phi\langle Mn\rangle^3 = 0 \tag{28}$$

differs from that of an unaggregated system by the presence of the bracketed term, which vanishes for a monodisperse distribution. The simultaneous solution of Eqs. (27) and (28) gives a compact and illuminating expression for the critical composition, namely,

$$\phi_c = [1 + \{\langle MN\rangle/(1+P^2)\}^{1/2}]^{-1}\,, \tag{29}$$

where P^2 measures the relative width of the distribution

$$P^2 = (\langle (Mn)^2\rangle - \langle Mn\rangle^2)/\langle Mn\rangle^2\,. \tag{30}$$

The critical composition can also be expressed in terms of the weight-average [Eqs. (26) and (27)] and "z-average" moment[36,37] $\langle Mn\rangle_z$,

$$\langle Mn\rangle_z = \sum_{n=1}^{\infty} (Mn)^2\phi_n \Big/ \sum_{n=1}^{\infty} (Mn)\phi_n \tag{31}$$

as

$$\phi_c = [1 + \langle Mn\rangle_w \langle Mn\rangle_z^{-1/2}]^{-1}\,. \tag{32}$$

The critical value of the mixing parameter χ is also essentially that for a system of particles of size $\langle Mn\rangle$:

$$\chi_c = [1 + \langle Mn\rangle^{1/2}]^2/2\langle Mn\rangle + [1 - (1+P^2)^{1/2}]^2/2\langle Mn\rangle^{1/2}(1+P^2)^{1/2} \tag{33a}$$

or

$$\chi_c = [1 + \langle Mn\rangle_w^{1/2}]^2/2\langle Mn\rangle_w + [\langle Mn\rangle_z^{1/2} - \langle Mn\rangle_w^{1/2}]^2/2\langle Mn\rangle_w\langle Mn\rangle_z^{1/2}\,. \tag{33b}$$

For fairly monodisperse size distributions, the critical composition is $\sim\langle Mn\rangle^{-1/2}$, and it is this feature of the model which allows for the extremely low critical compositions of aggregated surfactant systems, despite the fact that ϕ_c for the unaggregated system would be as large as $O(M^{-1/2})$.

These results given in Eqs. (32) and (33) agree with those of Stockmayer[36] and of Koningsveld and Staverman[37] for multicomponent nonassociating solutions described by the Flory–Huggins free energy, and as shown explicitly in the latter work, they may be derived from the general determinental relations of Gibbs for the spinodal and critical point.

III. CRITICAL MICELLE CONCENTRATION

In the limit of extremely low surfactant concentration, the free energy gain due to aggregation of amphiphiles is outweighed by the associated loss of translational entropy, and the extent of aggregation is thus negligible. At larger ϕ, aggregation becomes appreciable, and this is shown in several ways in Fig. 2. First, the osmotic pressure[38] displays a knee at $\phi_{\rm cmc}$ since, in the dilute limit, it is sensitive to the number of entities in solution which translate as distinct particles, rather than to the total number of surfactant molecules. Second, the mean aggregate size $\langle n\rangle$ increases rather sharply, and finally, most of the added surfactant above that at $\phi_{\rm cmc}$ is incorporated into aggregates and therefore does not change the monomeric amphiphile concentration ϕ_1 appreciably.

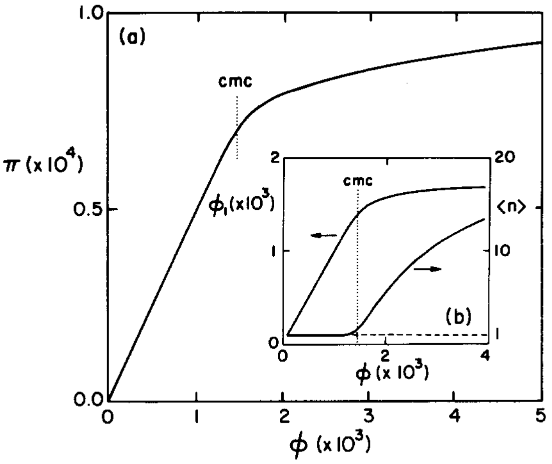

FIG. 2. Solution properties near the onset of aggregation, with parameters as in Fig. 1. (a) The reduced osmotic pressure as a function of surfactant volume fraction deviates from the ideal linear behavior at the critical micelle concentration (dotted). Inset (b) shows the concentration dependence of the monomer volume fraction and mean aggregation number.

For typical values of the parameters ϵ and σ, the size distribution function displays a bimodal form, as shown in Fig. 3(a). Since the surface area per surfactant decreases with increasing aggregation number n, larger values of the surface energy term σ favor larger micelles, thus shifting the approximately Gaussian peak of the distribution function to larger n. Increasing ϵ shifts to smaller values the composition at which significant aggregation occurs, without varying appreciably the mean micelle size observed at high concentration [Fig. 3(b)]. The fairly gradual increase in aggregate size with concentration, far above the cmc, is consistent with recent interpretations of neutron scattering experiments on solutions of alkyl polyoxyethylene ethers.[2]

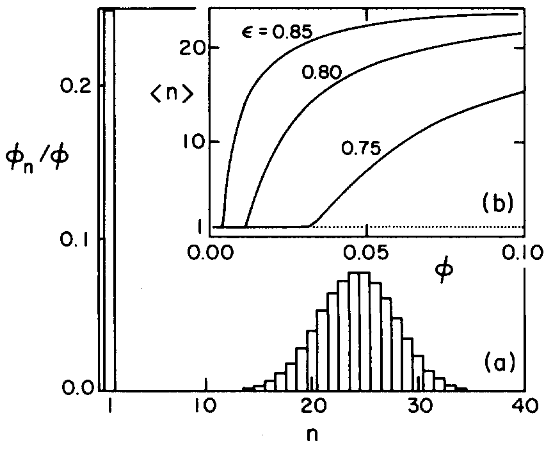

FIG. 3. (a) Micelle size distribution for $\phi = 0.08$, $M = 20$, $\epsilon = 0.85$, and $\sigma = 3$. (b) Composition dependence of mean aggregation number, with parameters as in (a), but varying ϵ, as indicated.

The bimodality of the distribution shown in Fig. 3 suggests a correspondence with an idealized two-state model[13] with monomers and aggregates of only a single size. Therefore, consider first the mathematical properties in this bidisperse limit, for which

$$\Delta_m = \begin{cases} \Delta & m = n \\ +\infty & m \neq n \end{cases}, \tag{34}$$

with $\Delta < 0$ to favor aggregation. When the surfactant concentration is very low, the reduced osmotic pressure becomes

$$\pi \approx \sum_{n=1}^{\infty} N_n/\Omega = \sum_{n=1}^{\infty} \phi_n/nM \tag{35}$$

or, using Eqs. (34) and (8),

$$\pi \approx \phi_1/M + \phi_n/nM = \phi_1/M + (\phi_1/M)^n e^{-\beta\Delta}. \tag{36}$$

The normalization of the distribution is

$$\phi = \phi_1 + nK_n(\phi_1)^n \quad (K_n = e^{-\beta\Delta}/M^{n-1}) \tag{37}$$

with K_n the "association constant" for the aggregation process. From the experimental point of view, ϕ is the variable under direct control, but Eqs. (36) and (37) are written in terms of the monomer concentration. The solution of Eq. (37) for ϕ_1 as a function of ϕ in closed form is not possible for arbitrary n, though, and as noted by Stillinger and Ben-Naim,[13] even the analytic inversion of a Taylor series expansion will break down whenever $d\phi/d\phi_1 = 0$. From Eq. (37) this condition is

$$1 + n^2K_n(\phi_1)^{n-1} = 0, \tag{38}$$

whose $n - 1$ solutions are distributed uniformly around a circle in the complex ϕ_1 plane, and are indexed by the integers $k = 1,2,...,n - 1$;

$$\phi_1^{(k)} = K_n^{-1/(n-1)} n^{-2/(n-1)} \exp[2\pi i(k - 1/2)/(n - 1)]. \tag{39}$$

Since these branch points exist only for complex values of monomer concentration (the solutions only coincide with the real axis in the limit $n \to \infty$), the composition variation of ϕ_1 is strictly analytic. Yet, as n increases, the singularities move closer together, and those indexed by $k = 1$ and $n - 1$ steadily approach the real axis, producing a $\phi_1(\phi)$ curve which has an ever more nearly discontinuous slope. This is reminiscent of the motion of the zeroes of the grand partition function, in the complex fugacity plane, as the thermodynamic limit is approached in a fluid or magnet.[14] In the limit $n \gg 1$, ϕ_1 varies linearly with ϕ for $\phi < |\phi_1^{(k)}|$, and very slowly, as $(\phi)^{1/(n-1)}$, far above it. The critical micelle concentration appears as the concentration at which $\phi_1 = |\phi_1^{(k)}|$. To deduce the behavior of the various thermodynamic functions in the neighborhood of this concentration, we note that the vanishing of $d\phi/d\phi_1$ at $\phi_1^{(k)}$ leaves the second derivative finite. Thus, an expansion for $\phi(\phi_1)$ starts out quadratically in $[\phi - \phi(\phi_1^{(k)})]$ so the expression for ϕ_1 has a square root singularity:

$$\phi_1 - \phi_1^{(k)} = \left[2 \left| \frac{d^2\phi(\phi_1^{(k)})}{d\phi_1^2} \right|^{-1} \right]^{1/2} \times [\phi - \phi(\phi_1^{(k)})]^{1/2} + \cdots. \tag{40}$$

Since only real values of ϕ are accessible experimentally, the small imaginary parts of the closest branch points to the real axis cause a rounding of the otherwise nonanalytic behavior in Eq. (40), a phenomenon which is conceptually quite similar to the rounding of the helix–coil transition of polypeptides: As shown by Li and Scheraga,[39] the fixed point of a renormalization-group transformation describing such a transition lies slightly off the real axis in the space of interaction parameters, so the observable physical behavior of the order parameter (fractional helicity) is strictly analytic.

Considering only these two branch points, the functional form of $\phi_1(\phi)$ depends on the quantity

$$[(\phi - \phi_{\rm cmc})^2 + \eta^2]^{1/2} + \cdots, \tag{41}$$

with η of order $1/n$. Sufficiently close to the cmc, this rounded square root dependence on surfactant concentration appears in all moments of the distribution function. Thus, the osmotic pressure and mean aggregation number, which are essentially the zeroth and first moments, respectively, have branch points in the complex ϕ_1 plane.

This type of analysis is clearly most appropriate to micelle models with size distributions narrowly peaked around some large size, like that in Fig. 3. To make connection with the ideal two-state model described above, we write the normalization condition for the complete distribution as

$$\begin{aligned} \phi &= \phi_1 + \sum_{n=2}^{\infty} \exp(-g_n), \\ -g_n &= -\beta\Delta_n + \ln(Mn) + n\ln(\phi_1/M). \end{aligned} \tag{42}$$

The function g_n may be interpreted as an effective free energy which includes the loss of entropy accompanying the restriction that the centers of mass of the monomers translate together. The characteristic behavior of this function, and the size distribution corresponding to it, are shown in Fig. 4. Clearly, a steepest-descent approximation should be valid for that part of the distribution near the region of the minimum at $n \approx 24$. Thus, we convert the summation in Eq. (42) to an integral, expand g_n to second order around its stationary point n_s which satisfies

$$-g_n' = -\beta\Delta_n' + 1/n + \ln(\phi_1/M) = 0, \tag{43}$$

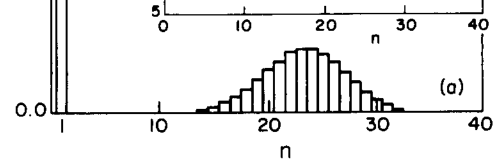

FIG. 4. (a) Micelle size distribution for $\phi = 0.005$, $\epsilon = 0.9$, and $\sigma = 3$. Inset (b) shows effective free energy of formation of micelles for $n > 2$.

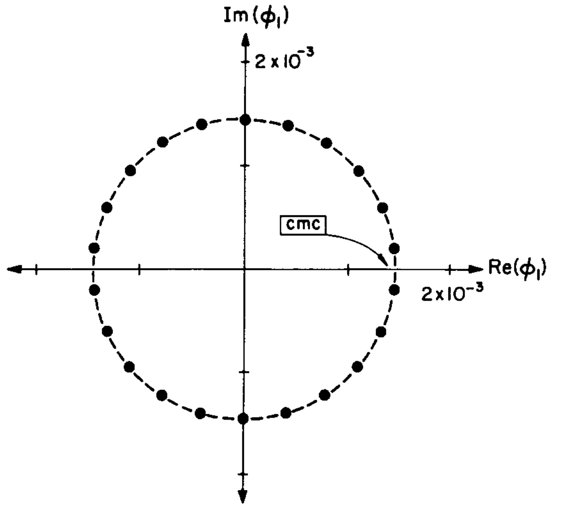

FIG. 5. Branch points in the complex monomer volume fraction plane at the self-consistently determined critical micelle concentration obtained in the Gaussian approximation map to the two-state aggregation model.

to obtain a Gaussian integral

$$\sum_{n=2}^{\infty} \exp[-g_n] \approx \exp[-g_{n_s}] \int_{-\infty}^{\infty} dn \times \exp[-\tfrac{1}{2} g''_{n_s}(n-n_s)^2] . \qquad (44)$$

The normalization condition then reduces to

$$\phi = \phi_1 + n_s M^{1-n_s} \exp[-\beta\Delta_{n_s}] \left[\frac{2\pi}{g''_{n_s}}\right]^{1/2} (\phi_1)^{n_s}. \qquad (45)$$

This is to be considered a *self-consistent* equation for ϕ_1, since n_s itself depends on ϕ_1 through Eq. (43). Note, however, that this dependence is weak, and ϕ_1 varies little in the cmc region, so that n_s is essentially constant there, as are the width parameters in Eq. (45) as a consequence.

Comparing Eqs. (37) and (45) it is clear that we have mapped the bimodal polydisperse model onto the two-state model, with a simple redefinition of the effective association constant K_n,

$$K_n \to K_n \left[\frac{2\pi}{\beta\Delta''_n + \dfrac{1}{n^2}}\right]^{1/2} \Bigg|_{n=n_s} \qquad (46)$$

so the analysis outlined above carries through as before.

As an example, Fig. 5 shows the branch points corresponding to the example in Fig. 4, where to determine n_s, we have chosen the nearest integer to that at the minimum of g_n. The critical micelle concentration deduced from this result is shown as the dotted lines in Figs. 2(a) and 2(b), and they clearly lie accurately in the region of greatest change of the various properties.

For aggregation models in which the micelle free energy results in sharply peaked bimodal distributions the above analysis suggests that the critical micelle concentration is larger than, and fairly unrelated to the concentration at which there is an inflection point in the size distribution, a criterion for the cmc which has been suggested by Ruckenstein and Nagarajan.[40] Indeed, at the critical micelle concentration itself, the distribution consists of monomer plus a small, although well defined, Gaussian peak at large n. The Ruckenstein–Nagarajan criterion provides a lower bound on the cmc.

IV. PHASE DIAGRAMS

In order to describe the details of the two-phase coexistence in the alkyl polyoxyethylene ether solutions, and in particular the presence of lower critical solution temperatures (LCSTs) and closed solubility loops, the temperature dependence of the mixing parameter χ must be specified. Various experimental methods[41] have revealed a lessening of the solvation of the ethylene oxide chains with increasing temperature, and this is plausibly interpreted as due to the thermal disruption of hydrogen bonds. Reentrant solubility is also found in solutions of homopolymers of ethylene oxide,[11] whose solubility in water is wholly attributable to hydrogen bonding. Thus, it appears that the LCSTs in the nonionic surfactant solutions are also due to such intermolecular hydrogen bonding, which by its geometrical constraints freezes out molecular orientational entropy and compensates for the increased mixing entropy as temperature is lowered. This mechanism is then identical to that which is believed[18–20] to underlie reentrant solubility in binary mixtures of comparable-size molecules. To describe the properties of such highly anisotropic potentials as hydrogen bonds, we employ a simple mean field theory[20] to arrive at an angle-averaged effective isotropic potential: Consider the usual prescription[42] for mapping a nonspherical intermolecular pair potential $u(r_{ij};\omega_i\omega_j)$, a function of the interparticle separation r_{ij} and the variables ω_i and ω_j which specify the molecular orientations, onto a spherically symmetric, but *temperature-dependent* potential $\bar{u}(r_{ij};T)$:

$$\exp[-\beta\bar{u}(r_{ij};T)] = \iint d\omega_i\, d\omega_j \exp[-\beta u(r_{ij};\omega_i,\omega_j)] , \qquad (47)$$

with a suitable normalization for the angular integrals. In a lattice model of a solution with only nearest-neighbor interactions, the only relevant interparticle distance is the lattice constant, so the distance dependence of u and $\bar{u}$ may be ignored. The phenomenological assumption we make, which is akin to that in the Zimm–Bragg[43] model for helix–coil transitions of polypeptides, is that for highly anisotropic potentials the integrals in Eq. (47) may be considered as a sum of two terms, arising from those parts of orientational phase space which correspond to the hydrogen bond, and those which do not. That is, we model the right-hand side of Eq. (47) by a two-level *orientational* partition function Z_{ij}, where

$$Z_{ij} = \omega^0 \exp[-\beta u^0] + \omega^* \exp[-\beta u^*] , \qquad (48)$$

where u^0 and u^* are, respectively, the van der Waals energy and hydrogen bond strength, and the factors ω^0 and ω^* reflect the relative volumes of orientational phase space corresponding to the two interactions. The geometric constraints on the hydrogen bond imply $\omega = \omega^*/\omega^0 \ll 1$. With Eq. (48), we generalize the energy parameter w in Eqs. (5) and (6) to[20]

$$-k_B T \ln[Z_{pp} Z_{ss}/(Z_{ps})^2] . \qquad (49)$$

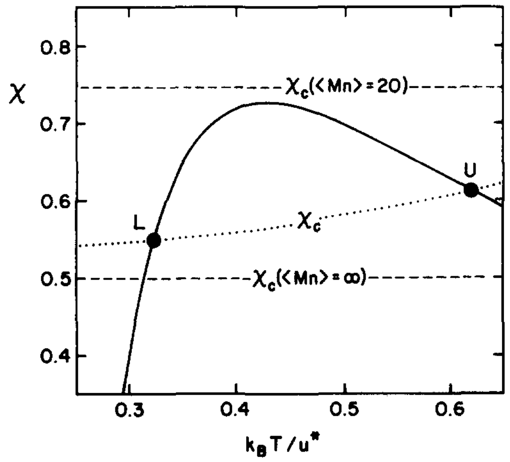

FIG. 6. Temperature dependence of the effective interaction parameter corresponding to a nonionic surfactant in a hydrogen-bonding solvent, with $|u^0/u^*| = 0.094$ and $\omega = 0.01$. The critical values of χ corresponding to systems of different aggregation numbers are indicated. Solid dots indicate the upper (U) and lower (L) critical solution points.

Perhaps the simplest model which will lead to lower critical solution points is one which treats only the solvent–surfactant hydrophilic group interaction as a two-level system, with all other orientational partition functions simply proportional to the exponential of a nearest-neighbor energy. This yields an effective mixing term of the form

$$\chi = -2d\{u^0/k_BT + \ln[1 + \omega \exp(u^*/k_BT)]\}, \qquad (50)$$

where $u^0 < 0$, $u^* > 0$, and $\omega \ll 1$.

Figure 6 shows the characteristic form of $\chi(T)$ in this approximation, for the case $|u^0/u^*| = 0.094$, $\omega = 0.01$. Also shown are the critical values of χ for systems of different mean aggregation number, indicating how, as the temperature is lowered and χ bends over toward the critical coupling at the upper consolute point, the true critical interaction (obtained from micelle free energy parameters described below) decreases according to Eqs. (33a) and (33b) as aggregation increases. Thus, the transition back to the one-phase region occurs at a lower temperature than that for the nearly unaggregated system near U.

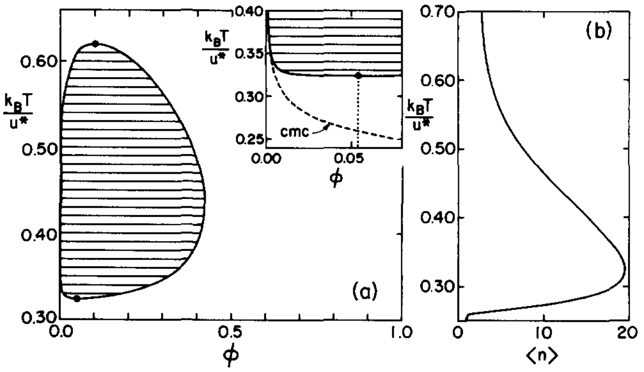

FIG. 8. Closed-loop phase diagram (a) and temperature variation of the mean aggregation number at the lower critical composition (b) for a nonionic surfactant in a hydrogen-bonding solvent. Inset in (a) shows the critical micelle concentration near the lower critical solution temperature (dashed), and the path of critical composition (dotted).

The large gain in hydrophobic free energy in the process of aggregation drives the total solution free energy of the micellar system below that for the unaggregated solution, as shown in Fig. 7, although the two free energies merge in the limit of infinite dilution, where the extent of aggregation vanishes. Referring again to Fig. 6, we see that in a range of temperatures, with appropriate parameters in χ, it is possible for the mixture to exist as a single stable phase, *in the absence of aggregation* $[\chi < \chi_c(\langle Mn\rangle = 20)]$, yet to become unstable upon aggregation $[\chi > \chi_c(\langle Mn\rangle)]$.

We show in Fig. 8 the calculated phase diagram for a nonionic surfactant of length $M = 20$, and with $\gamma/k_B = 900$ K. For the purpose of illustration, we have chosen the temperature dependence of the hydrophobic free energy to be as discussed in Sec. II A, with $a/k_B = 30$ K, and $b/k_B = 0.9$, which thus represents a small enthalpic contribution disfavoring aggregation, and a large, compensating entropic term for the typical temperatures encountered in experiments. The micelle size distributions at $\phi = 0.2$ and two temperatures, above the UCST and below the LCST, shown in Figs.

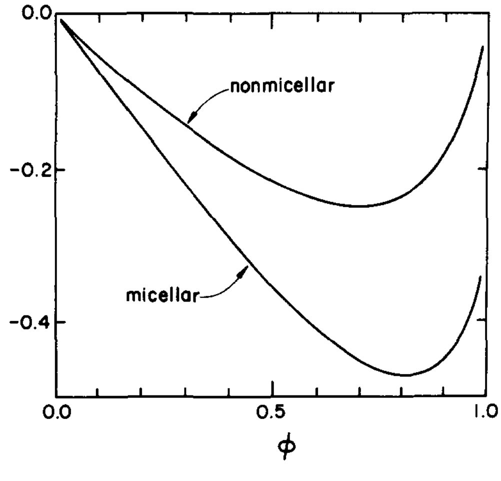

FIG. 7. Free energy of surfactant systems with and without micelle formation.

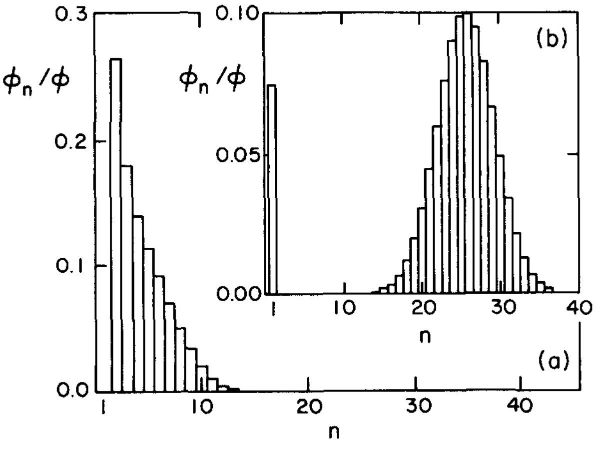

FIG. 9. Micelle size distributions above the upper critical solution temperature (a) and below the lower CST (b) for the system shown in Fig. 8.

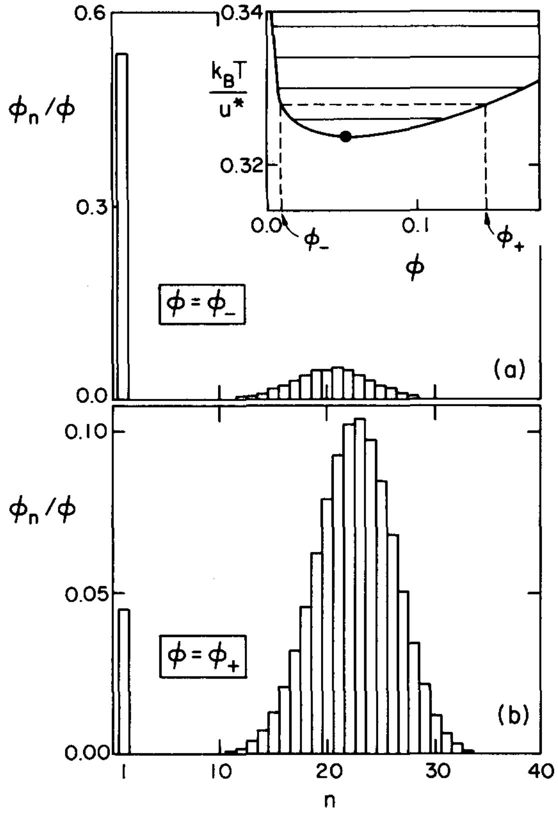

FIG. 10. Detail of region near the lower critical solution temperature in Fig. 8 and size distributions in the coexisting phases (ϕ_+) and (ϕ_-) at temperature indicated by the dotted line in the inset. Note the fractionation of larger micelles into the surfactant-rich phase.

9(a) and 9(b) indicate that near the upper critical solution temperature the most significant aggregation is into dimers, so that the upper critical composition is not much changed from that of a simple polymer solution with $M = 20$. In contrast, near the lower consolute point aggregation is significant, so the critical point is at a much lower volume fraction, according to Eqs. (29) and (32). These features are in agreement with the phase diagrams of a number of nonionic surfactants.[5,6]

The fractionation of larger micelles into the surfactant-rich phase is indicated in the detail of the region near the lower critical point shown in Fig. 10, and is qualitatively similar to that seen in theories of heterogeneous, but nonassociating polymer solutions.[44] Note also that the decreasing favorability of the hydrophobic energy h with decreasing temperature shifts the critical micelle concentration to larger values with decreasing temperatures below the LCST, also in qualitative agreement with experiment.[2] This shift in the cmc suggests an explanation for the small amount of micellar *growth* with temperature which has been inferred from neutron-scattering data.[2,3] In general, increasing temperature should certainly favor the dissociation of the aggregates simply through entropic effects. When $d\phi_{\rm cmc}/dT < 0$, however, a path of fixed composition and increasing temperature probes deeper into the region of saturating micellar growth [Fig. 3(b)], so that over a range of temperature, the mean aggregation number increases. At still higher T, though, the entropic effects dominate, and $\langle Mn \rangle$ decreases. Figure 8(b) shows the temperature dependence of $\langle n \rangle$ at the lower critical composition, illustrating this phenomenon.

While there is a very clear separation between the critical micelle concentration and the consolute point itself, the surfactant-poor branch of the coexistence curve may approach and even cross the cmc at temperatures far above the lower critical point. Then the two-phase equilibrium would involve micellar and nonmicellar solutions, rather than simply two solutions of different size micelles.

With larger surfactants it is possible, within the present model, to obtain critical compositions as low as $\phi \approx 0.015$ but the extraordinarily low critical compositions for certain alkyl polyoxyethylene ethers ($\sim 0.5\%$–1%) would seem to imply aggregation numbers which are inconsistent with a spherical micelle geometry. It thus seems likely that extended growth into shapes such as rods or disks may play a role at low temperatures and high surfactant concentrations.[8]

V. MICELLES AND MICROEMULSIONS

Widom[24] has described a phenomenological free energy for microemulsions which is based on the earlier work of Talmon and Prager,[21] as later modified by de Gennes *et al.*[22,23] In this model, a three-component microemulsion (oil + water + surfactant) is imagined to consist of microdomains of oil and water surrounded by a surfactant film, and the solution free energy consists of the entropy of mixing of those domains, and terms which account for the properties of the surfactant film and the interactions at the interfaces between unlike domains. In this section, we note a strong correspondence between the form of the free energy of the model microemulsion and that of the micellar solutions of nonionic surfactants studied in the present work. In particular, a simplified version of the latter, in which the micelles are assumed to be monodisperse, is studied to elucidate the consequences of treating domain size (i.e., micelle aggregation number) as a *variational parameter*, as was done in the model microemulsion and in the study of Leibler, Orland, and Wheeler,[10] as contrasted with applying an extremization condition to the free energy in terms of the *size distribution function*, yielding a mass action relation. We refer to these as "variational" and "aggregation" approaches, respectively.

Consider the free energy density of a monodisperse micellar solution, which may be written according to the discussion in Sec. II as

$$f = F/\Omega = k_BT\,[(1-\phi)\ln(1-\phi) + (\phi/Mn)\ln(\phi/Mn)] + (\phi/Mn)\Delta_n\,. \tag{51}$$

Here, Δ_n is, as before, the internal free energy of the micelles relative to isolated monomers, and we have assumed that all of the surfactant is present in the form of n-mers, just as all of the surfactant in the microemulsion is assumed to reside at the surface of the monodisperse microdomains, each of which is taken to be a cube of length ξ. From the definition of the domain sizes in the two models, we draw the correspon-

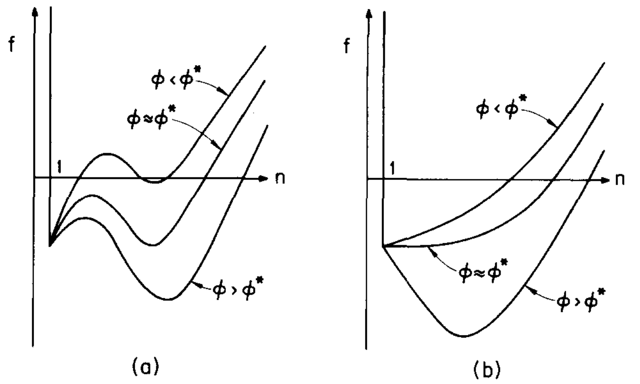

FIG. 11. Schematic illustration of size dependence of the effective free energy of domain formation for three concentrations of surfactant. In (a) a first order transition occurs as the surfactant concentration is increased past ϕ^*, while a second-order transition is shown in (b).

dence

$$(\text{micelles})\ Mna^3 \leftrightarrow \xi^3 \quad (\text{microemulsion domains})\,. \tag{52}$$

In Eq. (51), the quantity Δ_n/Mn is the free energy density within the micelles, and both in the model we considered in previous sections and in the model microemulsion that function has the same qualitative dependence on domain size: At small aggregation numbers the surface energy density is the dominant factor, rising with decreasing n in proportion to $n^{-1/3}$ for the micelles and with decreasing ξ as ξ^{-1} in the microemulsion, thus creating a barrier for the formation of small domains. At larger sizes this free energy density rises again, either due to polymer chain entropy effects in the micelles or to interface curvature energy in the microemulsion. In both of these systems there is thus some preferred large aggregate size (n_0 or ξ_0), which, in the absence of effects from the entropy of mixing, will be that which is observed, since it is also the solution to an extremization condition on the free energy,

$$\partial f/\partial n|_{n_0}=0 \quad \text{or} \quad \partial f/\partial \xi\,|_{\xi_0}=0\,, \tag{53}$$

as well as being a global minimum of f. Upon introducing the entropy of mixing term, this minimum at n_0 is shifted to a somewhat lower value. In addition, it is readily seen that for sufficiently small and fixed ϕ the term proportional to $\ln(\phi)/Mn$ lowers the free energy at $n=1$ below that near the isolated-domain minimum at $n\approx n_0$. This is shown in Fig. 11(a), where we envision varying the total surfactant concentration ϕ, from below to above the composition ϕ^* at which the two minima are equal in depth. In a variational approach in which the system chooses that value of n with the lowest free energy, we must introduce a *cutoff* at $n=1$, for the system would otherwise be unstable toward collapse into unphysically small values of n. This is identical with the conclusion reached by Widom[24] for the microemulsions, in which the contribution to the free energy density from the entropy of mixing of the microdomains varied as ξ^{-3}, thus necessitating a cutoff in ξ at a microscopic length a. Note, however, that while the minima at $n=1$ and $n\approx n_0$ (or $\xi=a$ and $\xi\approx\xi_0$) compete, the former is in general not the solution to the stationarity condition [Eq. (53)] which holds at the latter. In some regions of the space of thermodynamic parameters, however, these two minima may coincide [Fig. 11(b)].

In the variational theory, the equilibrium domain size remains at $n=1$ for all values of ϕ up to ϕ^*, and there will then be a transition to the state characterized by the value of $n\approx n_0$. If, as shown in Fig. 11(a), the latter minimum is at a value of n which is greater than unity, then this transition will be first order. If the two minima coincide [Fig. 11(b)], it will be second order. This is to be contrasted with the results which would be obtained if one considered an equilibrium between domains of size $n=1$ and larger, according to a mass action expression like that in Eq. (8). In such an equilibrium approach, there is no particular significance to the composition at which the effective free energy depth of n-mers equals that of monomers; the equilibrium free energy is continuously differentiable there, and the domain size is likewise a smooth function of the thermodynamic conditions. In the case $n_0>1$, the region of concentration at which the first order transition is predicted in the variational theory corresponds to, but is larger than the critical micelle concentration in the aggregation approach.

The model microemulsion predicts[24] that the equilibrium between the microemulsion phase, characterized by a large domain size, and a normal phase, with a microscopic cell size, is associated with a tricritical point, rather than an ordinary critical point as observed in experiments on three-component systems.[15,16] This tricritical point is itself associated with a locus of second-order transitions which are just those we discussed above, illustrated in Fig. 11(b). Since these transitions are absent in a theory which invokes an equilibrium between domain sizes, a reinterpretation of the model microemulsion within an aggregation approach may therefore be a fruitful line of investigation in the theory of microemulsions.[45]

VI. DISCUSSION

In this paper we have explored the predictions of a simple model for the formation of micelles and the equilibrium between two micellar phases. A particular emphasis was placed on the role of the aggregation in determining the extreme asymmetry of the coexistence curve in the temperature-composition phase diagram, and toward that end the entropy of mixing was estimated in an approximation equivalent to that in polymer solution theory. The determination of an appropriate form for this contribution to the free energy certainly warrants further attention, for the relationship between moments of the micelle size distribution and the coexistence curve properties depends sensitively upon the form of the entropy of mixing.[8] Central to this is an adequate description of excluded-volume effects, which in the present work are only accounted for on a phenomenological level analogous to that in the van der Waals equation of state. These finite-aggregate-size effects assume even more importance if one is to understand the various liquid–crystalline phases, and in particular the hexagonal phases, which appear to be composed of rod-like micelles. As recent work[46] has shown, the entropic effects associated with anisotropic excluded-volume interactions can be sufficient to drive a transition to a liquid crystal, and to influence strongly the size distribution of aggregates. Also, as mentioned in Sec. IV, it seems likely that very large, and hence nonspherical, aggregates play a role even at the critical point of some of the polyoxyethylenes, as evidenced by their extremely low critical compositions.

It thus becomes important to consider the evolution of micellar shapes from spheres to rods, say, as the total surfactant concentration is increased. The present model can account for this through the assumption that micelles larger than a certain characteristic aggregation number n_c assume a cylindrical form, with spherical caps. The chemical potential increment for the addition of monomers into the cylindrical region would then be roughly independent of total aggregation number.[47] With this simplifying approximation, the normalization summation for $n > n_c$ may be performed analytically, since it reduces to a geometric series. The value of n_c may be determined by the condition that the free energy density for a spherical micelle of n_c surfactants equal that in the cylinder. This extension of the model is currently being explored.

In estimating the effects of surfactant elongation on the internal entropy of the micelles, we invoked a highly idealized picture of the hydrocarbon chains, one which ignores the important excluded-volume effects present in real polymers. In addition, the validity of Gaussian random walk statistics for short polymers is certainly questionable, but it appears likely that the gross features of the entropic loss are captured in that approximation. In the present study, we have assumed perhaps the simplest forms for the temperature dependences of the micellar free energy parameters, consistent with the observed features of the coexistence curve and critical micelle concentration. A more detailed microscopic understanding will be necessary in order to correlate the micelle sizes and phase diagrams of the homologous series of compounds C_iE_j. Further, the intermicellar interactions must be treated more realistically, by accounting for spatial correlations and fluctuations, if the apparent lack of universality of the critical behavior[2] of these solutions is to be understood.

ACKNOWLEDGMENTS

It is a pleasure to thank G. B. Benedek, D. Blankschtein, and G. M. Thurston for an introduction to this problem, and for many important insights. The valuable comments of N. W. Ashcroft and B. Widom, and conversations with M. E. Cates, J. C. Lang, and C. Toprakcioglu are most appreciated. This work has been supported in part by a graduate fellowship from the Fannie and John Hertz Foundation, and by NSF, through Grant No. DMR-84-15669.

[1] For a review of theory and experiments on micellar systems, see (a) H. Wennerström and B. Lindman, Phys. Rep. **52**, 1 (1979); (b) *Surfactants in Solution*, edited by K. L. Mittal and B. Lindman (Plenum, New York, 1984), Vols. 1–3, and references therein.

[2] M. Corti, V. Degiorgio, and M. Zulauf, Phys. Rev. Lett. **48**, 1617 (1982); M. Corti, C. Minero, and V. Degiorgio, J. Phys. Chem. **88**, 309 (1984); M. Corti, V. Degiorgio, J. B. Hayter, and M. Zulauf, Chem. Phys. Lett. **109**, 579 (1984); V. Degiorgio, R. Piazza, M. Corti, and C. Minero, J. Chem. Phys. **82**, 1025 (1985); M. Zulauf, K. Weckström, J. B. Hayter, V. Degiorgio, and M. Corti, J. Phys. Chem. **89**, 3411 (1985).

[3] L. J. Magid, R. Triolo, and J. S. Johnson, Jr., J. Phys. Chem. **88**, 5730 (1984); R. Triolo, L. J. Magid, J. S. Johnson, Jr., and H. R. Child, *ibid.* **86**, 3689 (1982).

[4] M. Zulauf and J. P. Rosenbusch, J. Phys. Chem. **87**, 856 (1983).

[5] G. J. Tiddy, Phys. Rep. **57**, 1 (1980); D. J. Mitchell, G. J. T. Tiddy, L. Waring, T. Bostock, and M. P. McDonald, J. Chem. Soc. Faraday Trans. 1 **79**, 975 (1983).

[6] J. C. Lang and R. D. Morgan, J. Chem. Phys. **73**, 5849 (1980).

[7] Phase equilibrium in these solutions has been studied within the context of decorated lattice models [J. C. Lang, in Ref. 1(b), p. 35], and continuum approaches [L. Reatto and M. Tau, Chem. Phys. Lett. **108**, 292 (1984)], although neither has treated the association equilibria explicitly.

[8] D. Blankschtein, G. M. Thurston, and G. B. Benedek, Phys. Rev. Lett. **54**, 955 (1985); G. M. Thurston, D. Blankschtein, M. R. Fisch, and G. Benedek, J. Chem. Phys. (in press); D. Blankschtein, G. M. Thurston, and G. Benedek (preprint, 1985).

[9] P. G. de Gennes, Solid State Phys. Suppl. **14**, 1 (1978).

[10] L. Leibler, H. Orland, and J. C. Wheeler, J. Chem. Phys. **79**, 3550 (1984).

[11] R. Kjellander, J. Chem. Soc. Faraday Trans. 2 **78**, 2025 (1982); R. Kjellander and E. Florin, J. Chem. Soc. Faraday Trans. 1 **77**, 2053 (1981).

[12] P. J. Flory, *Principles of Polymer Chemistry* (Cornell University, Ithaca, NY, 1953).

[13] F. H. Stillinger and A. Ben-Naim, J. Chem. Phys. **74**, 2510 (1981).

[14] C. N. Yang and T. D. Lee, Phys. Rev. **87**, 404 (1952); T. D. Lee and C. N. Yang, *ibid.* **87**, 414 (1952).

[15] M. Kahlweit, E. Lessner, and R. Strey, J. Phys. Chem. **87**, 5032 (1983); **88**, 1937 (1984); **89**, 163 (1985).

[16] M. Kahlweit, R. Strey, P. Firman, and D. Haase, Langmuir **1**, 281 (1985).

[17] J. S. Huang and M. W. Kim, Phys. Rev. Lett. **47**, 1462 (1981); B. H. Robinson, C. Toprakcioglu, J. C. Dore, and P. Chieux, J. Chem. Soc. Faraday Trans. 1 **80**, 13 (1984); C. Toprakcioglu, J. C. Dore, B. H. Robinson, A. Howe, and P. Chieux, *ibid.* **80**, 413 (1984); O. Abillon, D. Chatenay, D. Langevin, and J. Meunier, J. Phys. (Paris) **45**, L223 (1984).

[18] J. D. Hirschfelder, D. Stevenson, and H. Eyring, J. Chem. Phys. **5**, 896 (1937); J. A. Barker and W. Fock, Discuss. Faraday Soc. **15**, 188 (1953); J. C. Wheeler, J. Chem. Phys. **62**, 433 (1975).

[19] R. E. Goldstein and J. S. Walker, J. Chem. Phys. **78**, 1492 (1983); J. S. Walker and C. A. Vause, *ibid.* **79**, 2660 (1983); R. E. Goldstein, *ibid.* **79**, 4439 (1983).

[20] R. E. Goldstein, J. Chem. Phys. **83**, 1246 (1985).

[21] Y. Talmon and S. Prager, Nature **267**, 333 (1977); Y. Talmon and S. Prager, J. Chem. Phys. **69**, 2984 (1978); **76**, 1535 (1982).

[22] P. G. de Gennes and C. Taupin, J. Phys. Chem. **86**, 2294 (1982).

[23] J. Jouffroy, P. Levinson, and P. G. de Gennes, J. Phys. (Paris) **43**, 1241 (1982).

[24] B. Widom, J. Chem. Phys. **81**, 1030 (1984).

[25] T. L. Hill, *Introduction to Statistical Thermodynamics* (Addison–Wesley, Reading, MA, 1960), Chap. 21.

[26] J. H. Hildebrand, J. Chem. Phys. **15**, 225 (1947).

[27] C. Tanford, *The Hydrophobic Effect*, 2nd ed. (Wiley, New York, 1980), and references therein.

[28] A. Ben-Shaul and W. M. Gelbart, J. Phys. Chem. **86**, 316 (1982); W. M. Gelbart, A. Ben-Shaul, W. E. McMullen, and A. Masters, *ibid.* **88**, 861 (1984).

[29] H. R. Kobraei, J. Chem. Phys. **81**, 6051 (1984).

[30] W. E. McMullen, W. M. Gelbart, and A. Ben-Shaul, J. Chem. Phys. **82**, 5616 (1985).

[31] H. S. Frank and M. W. Evans, J. Chem. Phys. **13**, 507 (1945).

[32] D. W. R. Gruen, J. Phys. Chem. **89**, 146 (1985); **89**, 153 (1985).

[33] Y. Chevalier and C. Chachaty, J. Phys. Chem. **89**, 875 (1985). See also Ref. 27.

[34] P. G. de Gennes, *Scaling Concepts in Polymer Physics* (Cornell University, Ithaca, NY, 1979), Chap. 1.

[35] J. A. Gualtieri, J. M. Kincaid, and G. Morrison, J. Chem. Phys. **77**, 521 (1982); K. A. Johnson, D. A. Johah, J. M. Kincaid, and G. Morrison, *ibid.* **82**, 5178 (1985).

[36] W. H. Stockmayer, J. Chem. Phys. **17**, 588 (1949).

[37] R. Koningsveld and A. J. Staverman, J. Polym. Sci. Part A 2, **6**, 325 (1968).

[38] For data on solution properties near the cmc of nonionic surfactant solutions see for example, J. M. Corkill, J. F. Goodman, and J. R. Tate, Trans. Faraday Soc. **60**, 996 (1964).

[39] Z. Li and H. A. Scheraga, J. Phys. Chem. **88**, 6580 (1984).

[40] E. Ruckenstein and R. Nagarajan, J. Phys. Chem. **79**, 2622 (1975); R. Nagarajan and E. Ruckenstein, J. Colloid. Interface Sci. **60**, 221 (1977). See also A. Ben-Naim and F. H. Stillinger, J. Phys. Chem. **84**, 2872 (1980).

[41] P. G. Nilsson and B. Lindman, J. Phys. Chem. **87**, 4756 (1983); P. G. Nilsson, H. Wennerström, and B. Lindman, *ibid.* **87**, 1377 (1983).

[42] G. S. Rushbrooke, Trans. Faraday Soc. **36**, 1055 (1940); J. S. Rowlinson, Mol. Phys. **52**, 567 (1984); G. O. Williams, J. L. Lebowitz, and J. K. Percus, J. Chem. Phys. **81**, 2070 (1984).

[43] B. H. Zimm and J. K. Bragg, J. Chem. Phys. **31**, 526 (1959). See also R. E. Goldstein, Phys. Lett. A **104**, 285 (1984).

[44] R. L. Scott M. Magat, J. Chem. Phys. **13**, 172 (1945); P. J. Flory, *ibid.* **12**, 425 (1944). See also Refs. 36 and 12.

[45] R. E. Goldstein and S. Leibler (to be submitted).

[46] W. E. McMullen, W. M. Gelbart, and A. Ben-Shaul, J. Chem. Phys. **82**, 5616 (1985).

[47] P. J. Missel, N. A. Mazer, G. B. Benedek, C. Y. Young, and M. C. Carey, J. Phys. Chem. **84**, 1044 (1980).